# $\mathcal{P}, \mathcal{T}$-odd effects for the RaOH molecule in the excited vibrational state

Anna Zakharova [*] and Alexander Petrov [†]

*St. Petersburg State University, St. Petersburg, 7/9 Universitetskaya Naberezhnaya 199034, Russia*
*and Petersburg Nuclear Physics Institute named by B.P. Konstantinov of National Research Centre "Kurchatov Institute," Gatchina, 1, Orlova roshcha 188300, Russia*

(Received 23 December 2020; accepted 17 February 2021; published 15 March 2021)

Triatomic molecule RaOH combines the advantages of laser coolability and the spectrum with close opposite-parity doublets. This makes it a promising candidate for experimental study of the $\mathcal{P}, \mathcal{T}$ violation. Previous studies concentrated on the calculations for different geometries without the averaging over the rovibrational wave function. The paper by V. Prasannaa *et al.* [Phys. Rev. A **99**, 062502 (2019)] claimed that the dependence of the $\mathcal{P}, \mathcal{T}$ parameters on the bond angle may significantly alter the observed value. We obtain the rovibrational wave functions of RaOH in the ground electronic state and excited vibrational state using the close-coupled equations derived from the adiabatic Hamiltonian. The potential surface is constructed based on the two-component relativistic coupled-cluster approximation with single, double, and perturbative triple excitation computations employing the generalized relativistic effective core potential for the radium atom. The averaged values of the parameters $E_{\text{eff}}$ and $E_s$ describing the sensitivity of the system to the electron electric dipole moment and the scalar-pseudoscalar nucleon-electron interaction are calculated and the value of $l$ doubling is obtained.

DOI: 10.1103/PhysRevA.103.032819

## I. INTRODUCTION

It is well known from the effects, such as mixing and decays of $K$ and $B$ mesons that symmetries under charge conjugation ($\mathcal{C}$), spatial reflection ($\mathcal{P}$), and time reversal ($\mathcal{T}$) are violated [1]. All $\mathcal{CP}$ (and, thus, $\mathcal{T}$) violation in the Standard model originates from the Cabibbo-Kobayashi-Maskawa and Pontecorvo-Maki-Nakagawa-Sakata mixing matrices in the quark and lepton interactions with $W^{\pm}$ bosons [2–5]. The other possible source of $\mathcal{CP}$ violation in the strong interaction is severely constrained and that constitutes the so-called strong $\mathcal{CP}$ problem [6,7]. Moreover, the explanation of the baryon asymmetry [8,9] in the universe may require new sources of the $\mathcal{CP}$ violation. The popular models of the new physics beyond the Standard model, such as various axion and supersymmetry scenarios predict new $\mathcal{CP}$-violating phenomena. Because of the small coupling constant of the weak interaction and cancellations due to the Glashow-Iliopoulos-Maiani mechanism, some effects, such as electron electric dipole moment (eEDM) turn out to be strongly suppressed in the Standard model compared to the expected new sources $\mathcal{CP}$ violation [10–13].

Although the searches of the new physics are popularly associated with collider experiments, the best limits on the eEDM come from high-precision atomic and molecular measurements [14,15]. This allows to put constraints on the new physics on the energies much higher than accessible on the accelerator experiments. Besides eEDM the same measurements permit the study of other $\mathcal{P}, \mathcal{T}$-violating phenomena, such as scalar-pseudoscalar nucleon-electron interaction [11,16,17], nuclear magnetic quadrupole moment [18], and interactions with new axionlike particles [19].

Some diatomic molecules with $\Omega = 1/2$ ($\Omega$ is projection of total momentum on molecular axis) that are promising for the $\mathcal{P}, \mathcal{T}$-odd interaction measurements, such as RaF [20,21], YbF [22], etc., permit their laser cooling. This allows to increase the coherence time by trapping the molecule and, as a result, improve the sensitivity of the experiment.

In turn, diatomic molecules with $\Omega = 1$ have closely spaced $\Omega$-doublet levels. The energy gap between levels of opposite parity for $\Omega = 1$ is much less than for $\Omega = 1/2$. Hence, polarization of $\Omega = 1/2$ requires much stronger electric fields that tends to increase systematic effects. Also it was shown previously that due to existence of $\Omega$-doublet levels the experiment on ThO [23–28] or $HfF^+$ [29,30] are very robust against a number of systematic effects.

Both the possibility of laser cooling and the existence of the close levels of the opposite parity can be realized with triatomic molecules, such as RaOH [31], YbOH [32], etc. In this case the role of the $\Omega$ doublets used in the diatomic molecular experiments is overtaken by the $l$ doublets [32,33]. Let us elucidate the nature of these levels and their importance for the search of $\mathcal{P}, \mathcal{T}$ violation.

The triatomic molecule with a linear equilibrium configuration possesses two bending modes on orthogonal planes. The superposition of oscillations in these two modes can be considered as a rotation of a bent molecule characterized by the rovibrational angular momentum $l$. Its eigenstates $|+l\rangle$ and $|-l\rangle$ are interchanged by the parity transformation $\mathcal{P}$. The energy eigenstates of a free molecule in absence of the external fields are also parity eigenstates $|\pm\rangle = \frac{1}{\sqrt{2}}(|+l\rangle \pm |-l\rangle)$. Because the bending modes in the two orthogonal planes are equivalent, the corresponding energy levels are degenerate. However, the Coriolis interaction with stretching

[*] zakharova.annet@gmail.com
[†] petrov_an@pnpi.nrcki.ru

 

modes results in the split of energies $\Delta E$ of $|\pm\rangle$ states known as $l$ doubling [32]. Since the dipole moment operator $\hat{d}_z$ is parity odd, its expectation values on the parity eigenstates $|\pm\rangle$ vanish. The parity symmetry is broken when the molecule is placed into the external electric field. The perturbed energy eigenstates $|E_\pm\rangle$ become superpositions of the parity eigenstates $|\pm\rangle$, and the corresponding energies are shifted because of the Stark effect. For sufficiently high electric fields $\mathcal{E} \gtrsim \frac{\hbar\Delta E}{d}$ (where $d = \langle l|\hat{d}_z|l\rangle$) the Stark effect changes from the quadratic regime to the linear one. At this point the energy eigenstates become, to a good degree, rovibrational momentum eigenstates $|\pm l\rangle$ and the molecule is fully polarized, i.e., the dipole moment expectation value reaches the maximum [33]. In absence of the $\mathcal{P}, \mathcal{T}$ violation, energy levels will not depend on the sign of the total angular momentum projection $M$ on the electrical field axis. Thus, the difference between energy shifts for $M = +1$ and $M = -1$ can be used to measure $\mathcal{P}$ and $\mathcal{T}$ violations. The maximum splitting is given by

$$2E_{\text{eff}}d_e + 2E_s k_s, \tag{1}$$

where $d_e$ is the value of the eEDM and $k_s$ is a characteristic dimensionless constant for scalar-pseudoscalar nucleon-electron interaction. To extract $d_e$ and $k_s$ from the measured splitting, one needs to know $E_{\text{eff}}$ and $E_s$ which are the subjects of molecular calculations [32,34–39].

Previous studies of triatomic molecules include the calculation of $E_{\text{eff}}$ and $E_s$ for different geometries of the molecules. However, the final number should be given by averaging over the rovibrational wave function that was not performed previously. In Ref. [38] the strong dependence of the $E_{\text{eff}}$ on the bond angle for the YbOH molecule was claimed to significantly affect the observed value. The quantum number $l$ can take values of $l = v, v-2, \ldots, 1(0)$, where $v$ is the quantum number for the bending mode. Thus, the lowest vibrational state with the $l$-doubling structure is the $v = 1$ level, which is of primary interest [32].

As the necessary electric field strength is proportional to the value of $l$ doubling, this parameter is important to estimate the applicability of the molecule.

The aim of this paper is to calculate $E_{\text{eff}}$ and $E_s$ for the lowest vibrational levels and $l$ doubling for $v = 1$.

## II. AVERAGING OVER THE NUCLEAR WAVE FUNCTION

In the Born-Oppenheimer approximation the total wave function of the molecule in Jacobi coordinates (Fig. 1) takes the form

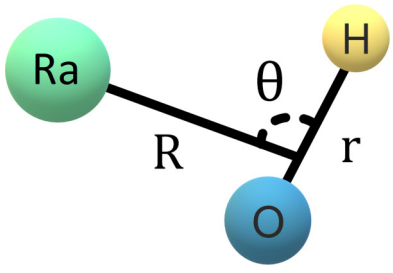


FIG. 1. Jacobi coordinates.

$$\Psi_{\text{total}} = \Psi_{\text{nuc}}(R, \hat{R}, \hat{r})\psi_{\text{elec}}(R, \theta|q), \tag{2}$$

$q$ means coordinates of the electronic subsystem, $\hat{r}$ and $\hat{R}$ are directions of the OH axis, and Ra—center mass of the OH axis, respectively, $\theta$ is the angle between the above axes, $R$ is Ra—center mass of OH separation. In the current approximation we fix the OH ligand stretch at the equilibrium distance $r = 1.832$ a.u. [40]. This is a reasonable approximation since the frequency of the OH vibrational mode is about one order of magnitude larger than other vibrational frequencies in RaOH.

The electronic wave function $\psi(R, \theta|q)$ is the solution of the multielectron Dirac-Coulomb equation in the field of the stationary classical nuclei. The Hamiltonian for the nuclear motion in the Jacobi coordinates with the fixed OH ligand stretch reads as

$$\hat{H}_{\text{nuc}} = -\frac{1}{2\mu}\frac{\partial^2}{\partial R^2} + \frac{\hat{L}^2}{2\mu R^2} + \frac{\hat{j}^2}{2\mu_{\text{OH}} r^2} + V(R, \theta), \tag{3}$$

where $\mu$ is the reduced mass of the Ra-OH system, $\mu_{\text{OH}}$ is the reduced mass of the OH ligand, $\hat{L}$ is the angular momentum of the rotation of the Ra-OH system around their center of mass, $\hat{j}$ is the angular momentum of the rotation of OH, and $V(R, \theta)$ is the effective adiabatic potential. The nuclear wave function $\Psi_{\text{nuc}}(R, \hat{R}, \hat{r})$ is the solution of the Schrödinger equation,

$$\hat{H}_{\text{nuc}}\Psi_{\text{nuc}}(R, \hat{R}, \hat{r}) = E\Psi_{\text{nuc}}(R, \hat{R}, \hat{r}). \tag{4}$$

To solve Eq. (4) we use expansion,

$$\Psi_{\text{nuc}}(R, \hat{R}, \hat{r}) = \sum_{L=0}^{L_{\max}} \sum_{j=0}^{j_{\max}} F_{JjL}(R)\Phi_{JjLM}(\hat{R}, \hat{r}), \tag{5}$$

where

$$\Phi_{JjLM}(\hat{R}, \hat{r}) = \sum_{m_L, m_j} C^{JM}_{Lm_L, jm_j} Y_{Lm_L}(\hat{R}) Y_{jm_j}(\hat{r}) \tag{6}$$

is coupled to the conserved total angular momentum $J$ basis set, $C^{JM}_{Lm_L, jm_j}$ are the Clebsch-Gordan coefficients, and $Y_{Lm_L}$ is spherical function. Due to parity conservation the sum $L + j$ must be even or odd for positive or negative parity, respectively.

The potential surface is expanded in terms of the Legendre polynomials,

$$V(R, \theta) = \sum_{k=0}^{k_{\max}} V_k(R) P_k(\cos\,\theta). \tag{7}$$

Substituting wave function (5) to Eq. (4) one gets the system of close-coupled equations for $F_{JjL}(R)$ [41]. We found that the solution is completely converged for $L_{\max} = j_{\max} = 20$ and $k_{\max} = 40$.

The eEDM and scalar-pseudoscalar nucleon-electron interaction on the molecule can be described by the $\mathcal{P}, \mathcal{T}$-odd Hamiltonian,

$$\hat{H}_{\not{\mathcal{P}}\not{\mathcal{T}}} = \hat{H}_d + \hat{H}_s, \tag{8}$$

$$\hat{H}_d = 2d_e \sum_i \begin{pmatrix} 0 & 0 \\ 0 & \boldsymbol{\sigma}_i \cdot \mathbf{E_i} \end{pmatrix}, \tag{9}$$

$$\hat{H}_s = ik_s \frac{G_F}{\sqrt{2}} \sum_{j=1}^{N_{\rm elec}} \sum_{I=1}^{N_{\rm nuc}} \rho_I(\vec{r}_j) Z_I \gamma^0 \gamma^5, \tag{10}$$

where $G_F$ is the Fermi constant, and $\rho_I$ is the charge density of the $I$th nucleon normalized to unity, $\mathbf{E_i}$ is the inner molecular electric field acting on the $i$th electron, and $\sigma$'s are the Pauli matrices.

Considering these interactions as a small perturbation their impact on the spectrum can be described by the expectation values of

$$E_{\rm eff}(R,\theta) = \frac{\langle \psi_{\rm elec}(R,\theta)|\hat{H}_d|\psi_{\rm elec}(R,\theta)\rangle}{d_e {\rm sgn}(\Omega)}, \tag{11}$$

$$E_s(R,\theta) = \frac{\langle \psi_{\rm elec}(R,\theta)|\hat{H}_s|\psi_{\rm elec}(R,\theta)\rangle}{k_s {\rm sgn}(\Omega)}, \tag{12}$$

on nuclear wave function (5),

$$E_{\rm eff} = \int dR\, d\hat{R}\, d\hat{r} |\Psi_{\rm nuc}(R,\hat{R},\hat{r})|^2 E_{\rm eff}(R,\theta), \tag{13}$$

$$E_s = \int dR\, d\hat{R}\, d\hat{r} |\Psi_{\rm nuc}(R,\hat{R},\hat{r})|^2 E_s(R,\theta). \tag{14}$$

## III. METHODS

We used the DIRAC 19 software package [42] to calculate molecular orbitals using the Dirac-Hartree-Fock self-consistent field (SCF) method as well as to construct the potential surface in the coupled-cluster approximation with single, double, and perturbative triple excitations [CCSD(T)]. The cc-pVTZ basis was employed for O and H atoms. To describe the electronic structure of the Ra atom we used a 10-valence electron basis with a generalized relativistic effective core potential (GRECP) [43–45] including spin-orbit interaction blocks that was developed by the PNPI Quantum Chemistry Laboratory [46].

The computations were performed for the molecular configurations corresponding to a grid of Jacobi coordinates. The values of $R$ were chosen to cover the span from 3.6 to 6.0 a.u. with step 0.2 a.u. The values of $\theta$ correspond to the zeros of Legendre polynomial $P_5$ and two angles for linear configurations, i.e., 0°, 25°, 57°, 90°, 122°, 155°, and 180°.

Spinors calculated using the GRECP have incorrect behavior in the core region. To restore the correct spinor functions, the method of one-center restoration based on equivalent bases, implemented in the MOLGEP program, was applied [47–49]. MOLGEP is restricted to the real two-component molecular orbitals. For this paper we developed the code that applies MOLGEP to compute the matrix elements on the complex orbitals in the Dirac quaternionic representation.

The orbitals obtained in Dirac were used to calculate the matrix elements of properties in MOLGEP. Convolution of the matrix elements computed on the molecular orbitals $\psi_i$ with the one-electron density-matrix $\rho_{ij}^{(1)}$ gives the average property value for the electron configuration,

$$\langle O \rangle = \frac{1}{N_{\rm elec}} \sum_{i,j=1}^{N_{\rm orb}} \rho_{ij}^{(1)} \langle \psi_i|\hat{O}|\psi_j\rangle. \tag{15}$$

The SCF density matrix in the basis of molecular orbitals was constructed based on the occupation: $\rho_{ij}^{(1)} = \delta_{ij}$ if both indices $i$, $j$ correspond to the occupied orbitals, and $\rho_{ij}^{(1)} = 0$ if any index correspond to the virtual orbital. The correlated single-electron density matrices were obtained for RaOH linear configurations using the CCSD method implemented in the MRCC software package [50]. This method was used to calculate the SCF values and the correlation corrections for the $\mathcal{P},\mathcal{T}$-odd parameters $E_{\rm eff}$ and $E_s$. Due to the restrictions of the Dirac-MRCC interface the correlation corrections were computed only for the linear configurations. Because of the small magnitude of these corrections (that at their maximum are 5% of the SCF value) we neglect their dependence on the angle and apply them to the nonlinear configurations.

The potential surface computed on a grid for each value of $R$ was interpolated by Akima splines and then expanded in terms of Legendre polynomials (7) with $k_{\rm max} = 40$. The coefficients $V_k(R)$ were then interpolated by Akima splines. The bicubic interpolation was applied to the values $E_{\rm eff}$ and $E_s$ computed on a grid. The interpolated functions were used to set up the close-coupled equations for $F_{Jjl}(R)$ by means of a code developed by the authors.

## IV. RESULTS AND DISCUSSION

The obtained potential surface is represented in Fig. 2. The minimum corresponds to $R = 4.4$ a.u. and $\theta = 0°$. The spectrum of the vibrational levels obtained from the solution of the close-coupled equations corresponds to the values of $\nu_1(\sigma^+) = 469$ and $\nu_2(\pi) = 363$ cm$^{-1}$ for the $^2\Sigma_{1/2}$ ground state. These values can be compared to $\nu_1(\sigma^+) = 437$ and $\nu_2(\pi) = 366$ cm$^{-1}$ computed in Ref. [31] by the multiconfigurational SCF method.

The difference between the energy levels of opposite parities and the same quantum numbers $J = 1$, $v = 1$ gives the value of $l$ doubling equal to 14.467 MHz. For the energy

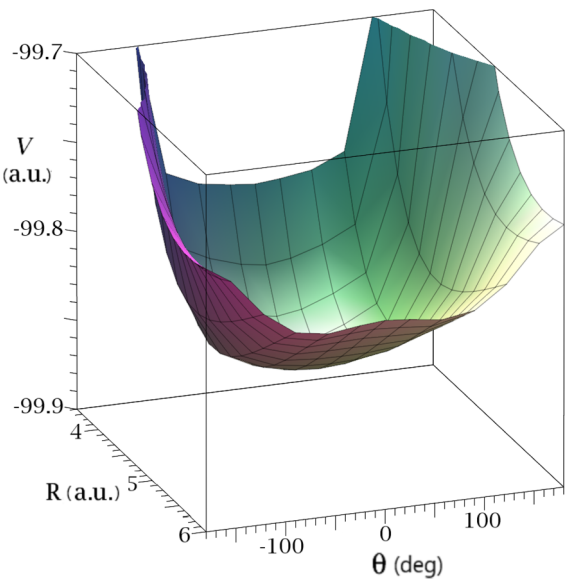


FIG. 2. RaOH potential surface $V(R,\theta)$ at the CCSD(T) level. The coordinates are introduced in Fig. 1.

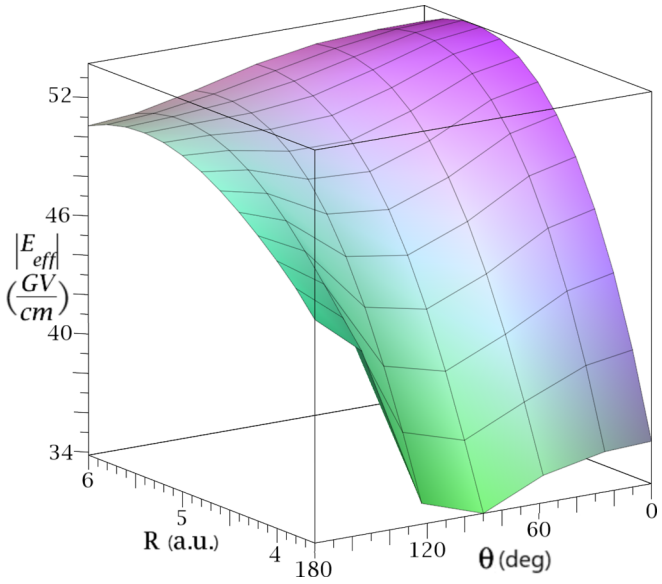


FIG. 3. Results for $E_{\text{eff}}(R, \theta)$ as a function of Jacobi coordinates at the CCSD level (the angular dependence of the correlation correction is neglected).

levels with $J = 2$, $v = 1$ we obtain the value of $l$-doubling 43.400 MHz which is three times larger. This is consistent with theoretical considerations that $l$ doubling is proportional to the factor $J(J + 1)$ and confirms the numerical stability of our computation.

The calculated for nonlinear configurations $E_{\text{eff}}(R, \theta)$ and $E_s(R, \theta)$ are represented in Figs. 3 and 4, respectively, and show a similar dependence of the parameters on the Jacobi coordinates. In Figs. 5 and 6 the results for linear configuration are given. We compare the values (13) and (14) averaged over the vibrational nuclear wave function to the values computed

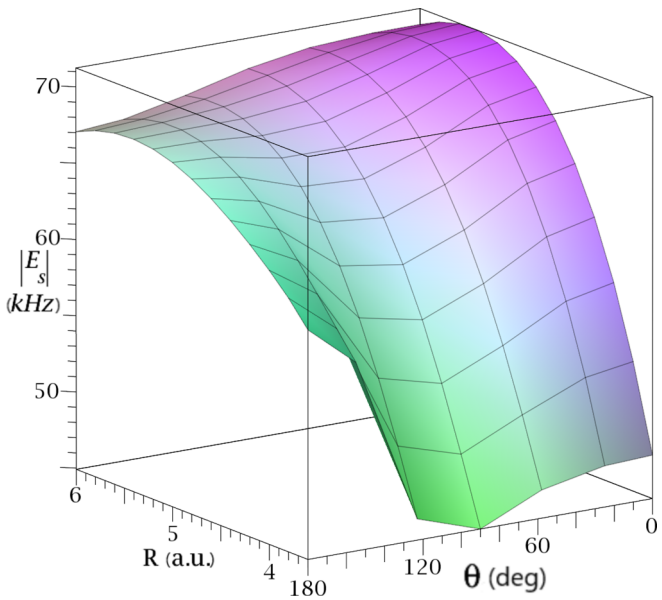


FIG. 4. Results for $E_s(R, \theta)$ as a function of Jacobi coordinates at the CCSD level (the angular dependence of the correlation correction is neglected).

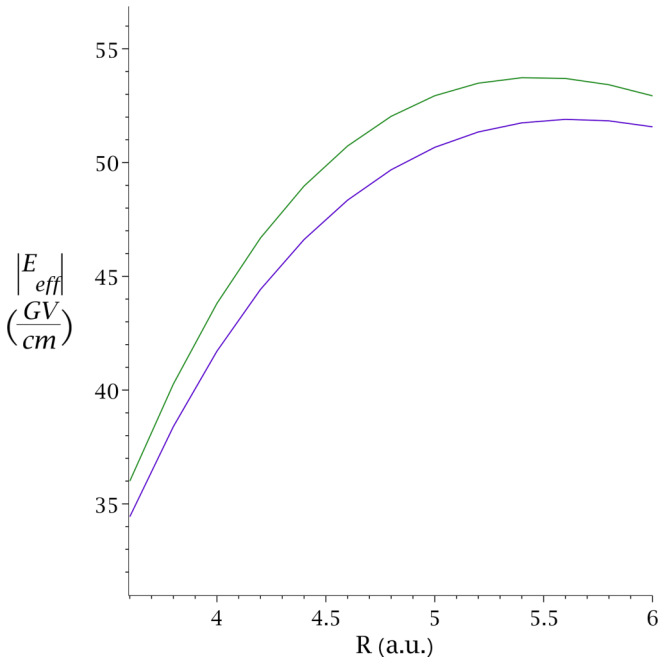


FIG. 5. $E_{\text{eff}}(R, \theta = 0)$ for RaOH calculated for linear configurations as a function of Ra-OH c.m. distance. The violet (lower) line corresponds to SCF values, and the green (upper) line takes into account the CCSD correction.

for the equilibrium configuration in Table I. It can be seen that the difference from the equilibrium values $E_{\text{eff}}$ and $E_s$ is 0.01% for $v = 0$ and 0.58% for $v = 1$. This means that the results obtained for the equilibrium configuration give

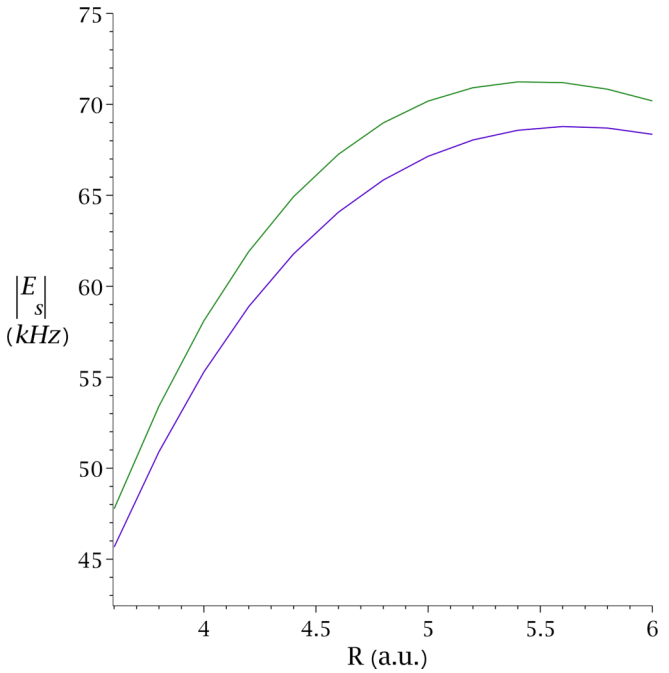


FIG. 6. $E_s(R, \theta = 0)$ for RaOH calculated for linear configurations as a function of Ra-OH c.m. distance. The violet (lower) line corresponds to SCF values and the green (upper) line takes into account the CCSD correction.

TABLE I. $\mathcal{P},\mathcal{T}$-odd parameters for the RaOH molecule.

| | $E_{\text{eff}}$, $\frac{\text{GV}}{\text{cm}}$ | $E_s$, (kHz) |
|---|---|---|
| Equilibrium | −48.866 | −64.788 |
| $v=0$ | −48.863 | −64.784 |
| $v=1$ | −48.585 | −64.416 |
| cGHF RaOH [39][a] | −56.2 | −75.6 |
| cGKS RaOH [39][b] | −49.3 | −66.4 |

[a] $\Omega = 0.494$.
[b] $\Omega = 0.471$.

a good approximation for the lowest vibrational levels. Our result does not confirm the expectations of Ref. [38] based on their YbOH computations that the dependence of the $\mathcal{P},\mathcal{T}$ parameters on the bond angle may significantly affect the observed value. This is consistent with the conclusions of Ref. [39] for the YbOH molecule where the estimate for the vibrational correction on the order of 0.1% was obtained for $v=1$ perturbatively in the bending angle with the nuclear wave function in the harmonic approximation. The values in Ref. [39] obtained using complex generalized Kohn-Sham (cGKS) show good agreement with our results.

## ACKNOWLEDGMENTS

The work was supported by the Russian Science Foundation Grant No. 18-12-00227. We thank I. P. Kurchavov for providing equivalent basis sets for the Ra atom used for the restoration procedure.

[1] I. B. Khriplovich and S. K. Lamoreaux, *CP Violation without Strangeness: Electric Dipole Moments of Particles, Atoms, and Molecules* (Springer-Verlag, Berlin, Heidelberg, 2012).
[2] M. Kobayashi and T. Maskawa, Prog. Theor. Phys. **49**, 652 (1973).
[3] Z. Maki, M. Nakagawa, and S. Sakata, Prog. Theor. Phys. **28**, 870 (1962).
[4] M. D. Schwartz, *Quantum Field Theory and the Standard Model* (Cambridge University Press, Cambridge, New York, 2014).
[5] Particle Data Group, P.-A. Zyla *et al.*, Prog. Theor. Exp. Phys. **2020**, 083C01 (2020).
[6] H.-Y. Cheng, Phys. Rep. **158**, 1 (1988).
[7] J. E. Kim and G. Carosi, Rev. Mod. Phys. **82**, 557 (2010).
[8] A. D. Sakharov, JETP Lett. **5**, 24 (1967).
[9] M. Dine and A. Kusenko, Rev. Mod. Phys. **76**, 1 (2003).
[10] T. Fukuyama, Int. J. Mod. Phys. A **27**, 1230015 (2012).
[11] M. Pospelov and A. Ritz, Phys. Rev. D **89**, 056006 (2014).
[12] Y. Yamaguchi and N. Yamanaka, Phys. Rev. Lett. **125**, 241802 (2020).
[13] Y. Yamaguchi and N. Yamanaka, Phys. Rev. D **103**, 013001 (2021).
[14] J. Baron, W. C. Campbell, D. DeMille, J. M. Doyle, G. Gabrielse, Y. V. Gurevich, P. W. Hess, N. R. Hutzler, E. Kirilov, I. Kozyryev *et al.*, Science **343**, 269 (2014).
[15] V. Andreev and N. Hutzler, Nature (London) **562**, 355 (2018).
[16] J. Ginges and V. V. Flambaum, Phys. Rep. **397**, 63 (2004).
[17] D. V. Chubukov and L. N. Labzowsky, Phys. Rev. A **93**, 062503 (2016).
[18] D. E. Maison, L. V. Skripnikov, and V. V. Flambaum, Phys. Rev. A **100**, 032514 (2019).
[19] D. Maison, V. Flambaum, N. Hutzler, and L. Skripnikov, Phys. Rev. A **103**, 022813 (2021).
[20] T. A. Isaev, S. Hoekstra, and R. Berger, Phys. Rev. A **82**, 052521 (2010).
[21] R. F. Garcia Ruiz, R. Berger, J. Billowes, C. L. Binnersley, M. L. Bissell, A. A. Breier, A. J. Brinson, K. Chrysalidis, T. E. Cocolios, B. S. Cooper *et al.*, Nature **581**, 396 (2020).
[22] J. Lim, J. R. Almond, M. A. Trigatzis, J. A. Devlin, N. J. Fitch, B. E. Sauer, M. R. Tarbutt, and E. A. Hinds, Phys. Rev. Lett. **120**, 123201 (2018).
[23] A. N. Petrov and L. V. Skripnikov, Opt. Spectrosc. **126**, 331 (2019).
[24] D. DeMille, F. B. an S. Bickman, D. Kawall, L. Hunter, D. Krause, Jr., S. Maxwell, and K. Ulmer, in *Art and symmetry in experimental physics*, edited by D. Budker, P. H. Bucksbaum, and S. J. Freedman, AIP Conf. Proc. No. 596 (AIP, New York, 2001), p. 72.
[25] A. N. Petrov, L. V. Skripnikov, A. V. Titov, N. R. Hutzler, P. W. Hess, B. R. O'Leary, B. Spaun, D. DeMille, G. Gabrielse, and J. M. Doyle, Phys. Rev. A **89**, 062505 (2014).
[26] A. C. Vutha, W. C. Campbell, Y. V. Gurevich, N. R. Hutzler, M. Parsons, D. Patterson, E. Petrik, B. Spaun, J. M. Doyle, G. Gabrielse *et al.*, J. Phys. B: At., Mol. Opt. Phys. **43**, 074007 (2010).
[27] A. N. Petrov, Phys. Rev. A **91**, 062509 (2015).
[28] A. N. Petrov, Phys. Rev. A **95**, 062501 (2017).
[29] W. B. Cairncross, D. N. Gresh, M. Grau, K. C. Cossel, T. S. Roussy, Y. Ni, Y. Zhou, J. Ye, and E. A. Cornell, Phys. Rev. Lett. **119**, 153001 (2017).
[30] A. N. Petrov, Phys. Rev. A **97**, 052504 (2018).
[31] T. A. Isaev, A. V. Zaitsevskii, and E. Eliav, J. Phys. B: At., Mol. Opt. Phys. **50**, 225101 (2017).
[32] I. Kozyryev and N. R. Hutzler, Phys. Rev. Lett. **119**, 133002 (2017).
[33] N. R. Hutzler, Quantum Sci. Technol. **5**, 044011 (2020),
[34] M. G. Kozlov and L. N. Labzowsky, J. Phys. B: At., Mol. Opt. Phys. **28**, 1933 (1995).
[35] M. S. Safronova, D. Budker, D. DeMille, D. F. Jackson Kimball, A. Derevianko, and C. W. Clark, Rev. Mod. Phys. **90**, 025008 (2018).
[36] T. Fleig, Phys. Rev. A **96**, 040502(R) (2017).
[37] M. Denis, P. A. Haase, R. G. E. Timmermans, E. Eliav, N. R. Hutzler, and A. Borschevsky, Phys. Rev. A **99**, 042512 (2019).
[38] V. S. Prasannaa, N. Shitara, A. Sakurai, M. Abe, and B. P. Das, Phys. Rev. A **99**, 062502 (2019).
[39] K. Gaul and R. Berger, Phys. Rev. A **101**, 012508 (2020).
[40] K.P.Huber and G.Herzberg, *Molecular Spectra and Molecular Structure. IV Constants of Diatomic Molecules* (Van Nostrand Reinhold, New York, 1979), p. 514.

[41] P. McGuire and D. J. Kouri, J. Chem. Phys. **60**, 2488 (1974).

[42] DIRAC, a relativistic *ab initio* electronic structure program, Release DIRAC19, written by A. S. P. Gomes, T. Saue, L. Visscher, H. J. A. Jensen, and R. Bast, with contributions from I. A. Aucar, V. Bakken, K. G. Dyall, S. Dubillard, U. Ekström, E. Eliav, T. Enevoldsen, E. Faßhauer, T. Fleig, O. Fossgaard, L. Halbert, E. D. Hedegård, B. Heimlich–Paris, T. Helgaker, J. Henriksson, M. Iliaš, Ch. R. Jacob, S. Knecht, S. Komorovský, O. Kullie, J. K. Lærdahl, C. V. Larsen, Y. S. Lee, H. S. Nataraj, M. K. Nayak, P. Norman, G. Olejniczak, J. Olsen, J. M. H. Olsen, Y. C. Park, J. K. Pedersen, M. Pernpointner, R. di Remigio, K. Ruud, P. Sałek, B. Schimmelpfennig, B. Senjean, A. Shee, J. Sikkema, A. J. Thorvaldsen, J. Thyssen, J. van Stralen, M. L. Vidal, S. Villaume, O. Visser, T. Winther, and S. Yamamoto (available at http://dx.doi.org/10.5281/zenodo.3572669, see also http://www.diracprogram.org) (2019).

[43] A. Titov and N. Mosyagin, Int. J. Quantum Chem. **71**, 359 (1999).

[44] N. S. Mosyagin, A. Zaitsevskii, and A. V. Titov, Int. Rev. At. Mol. Phys. **1**, 63 (2010).

[45] N. S. Mosyagin, A. V. Zaitsevskii, L. V. Skripnikov, and A. V. Titov, Int. J. Quantum Chem. **116**, 301 (2016).

[46] URL: http://www.qchem.pnpi.spb.ru/Basis/, GRECPs, and basis sets.

[47] A. N. Petrov, N. S. Mosyagin, T. A. Isaev, A. V. Titov, V. F. Ezhov, E. Eliav, and U. Kaldor, Phys. Rev. Lett. **88**, 073001 (2002).

[48] A. V. Titov, N. S. Mosyagin, A. N. Petrov, T. A. Isaev, and D. P. DeMille, in *Recent Advances in the Theory of Chemical and Physical Systems*, edited by J.-P. Julien, J. Maruani, D. Mayou, S. Wilson, and G. Delgado-Barrio, Progress in Theoretical Chemistry and Physics, Vol 15 (Springer, Dordrecht, 2006), pp. 253–283.

[49] L. V. Skripnikov and A. V. Titov, Phys. Rev. A **91**, 042504 (2015).

[50] M. Kállay, P. R. Nagy, D. Mester, Z. Rolik, G. Samu, J. Csontos, J. Csóka, P. B. Szabó, L. Gyevi-Nagy, B. Hégely, I. Ladjánszki, L. Szegedy, B. Ladóczki, K. Petrov, M. Farkas, P. D. Mezei, and Á. Ganyecz, The MRCC program system: Accurate quantum chemistry from water to proteins, J. Chem. Phys. **152**, 074107 (2020). MRCC, a quantum chemical program suite. See www.mrcc.hu.